



THE UNIVERSITY *of* EDINBURGH

Edinburgh Research Explorer

## CONCRETE CONFINEMENT WITH TRM VERSUS FRP JACKETS AT ELEVATED TEMPERATURES

**Citation for published version:**

Cerniauskas, G, Tetta, Z, Bournas, D & Bisby, L 2020, 'CONCRETE CONFINEMENT WITH TRM VERSUS FRP JACKETS AT ELEVATED TEMPERATURES', *Materials and structures*, vol. 53, 58.  
<https://doi.org/10.1617/s11527-020-01492-x>

**Digital Object Identifier (DOI):**

[10.1617/s11527-020-01492-x](https://doi.org/10.1617/s11527-020-01492-x)

**Link:**

[Link to publication record in Edinburgh Research Explorer](#)

**Document Version:**

Peer reviewed version

**Published In:**

Materials and structures

**General rights**

Copyright for the publications made accessible via the Edinburgh Research Explorer is retained by the author(s) and / or other copyright owners and it is a condition of accessing these publications that users recognise and abide by the legal requirements associated with these rights.

**Take down policy**

The University of Edinburgh has made every reasonable effort to ensure that Edinburgh Research Explorer content complies with UK legislation. If you believe that the public display of this file breaches copyright please contact [openaccess@ed.ac.uk](mailto:openaccess@ed.ac.uk) providing details, and we will remove access to the work immediately and investigate your claim.



# CONCRETE CONFINEMENT WITH TRM VERSUS FRP JACKETS AT ELEVATED TEMPERATURES

G. Cerniauskas <sup>1</sup>, Z. Tetta <sup>2</sup>, D.A. Bournas <sup>3\*</sup> and L.A. Bisby <sup>1</sup>

<sup>1</sup> Institute for Infrastructure and Environment, School of Engineering, The University of Edinburgh, UK.

Email: luke.bisby@ed.ac.uk

<sup>2</sup> Former PhD Student, The University of Nottingham UK. Current: WSP Engineering Consulting, UK.

<sup>3</sup> European Commission, Joint Research Centre (JRC), Ispra, Italy.

\* Corresponding author. Email: [Dionysios.BOURNAS@ec.europa.eu](mailto:Dionysios.BOURNAS@ec.europa.eu)

## ABSTRACT

Despite the clear cost, ease of installation, and construction schedule advantages of confinement of concrete structural elements with fibre-reinforced polymers (FRPs) for strength and deformability enhancement, concerns as to their performance at elevated temperature, or in fire, remain. The results of a series of elevated temperature experiments on FRP and textile reinforced mortar (TRM) strengthening systems for confinement of circular concrete columns are presented. The behaviour and effectiveness of the respective confining systems is studied up to temperatures of 400°C. A total of 24 concrete cylinders were wrapped in the hoop direction with different amounts of FRP or TRM, heated to steady-state temperatures between 20 and 400°C, and loaded to failure in concentric axial compression under a steady-state thermal regime. The results indicate that the effectiveness of the FRP confining system bonded with epoxy decreased considerably, but did not vanish, with increasing temperatures, in particular within the region of the glass transition temperature of the epoxy resin/adhesive. Conversely, the TRM confining system, bonded with inorganic mortar rather than epoxy, demonstrated superior performance than the FRP confining system at 400°C as compared against tests performed at ambient temperature.

## KEYWORDS

FRP, textile reinforced mortar, TRM, strengthening, high temperature, fire, confinement.

## INTRODUCTION AND BACKGROUND

A popular application of fibre reinforced polymers (FRPs) is strengthening concrete columns by confinement with FRP in the hoop direction (Bisby *et al.* 2011). However, the performance of FRP systems at elevated temperatures is potentially problematic since much of their strength, stiffness, and bond properties are lost at temperatures that are rapidly exceeded in building fires (Chowdhury *et al.* 2011). Carbon fibres used in FRP systems may be capable of resisting temperatures of more than 800°C; however, epoxies used to bond the fibres and adhere FRP systems to concrete lose a considerable proportion of their mechanical properties at temperatures as low as 60°C-82°C (ACI 2008). These reductions in mechanical properties can be expected in the region of the epoxy's glass transition temperature ( $T_g$ ) as it changes from hard and brittle to soft and plastic. Testing has been carried out previously to investigate the performance of FRP confining systems for concrete columns during standard fire exposures (e.g. Chowdhury *et al.* 2007) and during both transient and steady-state heating to elevated temperatures (Rickard *et al.* 2013). This testing has shown that considerable (about 50%) loss of effectiveness of the FRP strengthening system occurred at temperatures as low as 15°C below the  $T_g$  of the epoxy adhesive, which is thought to be due to reductions in the tensile strength and stiffness of the FRP wraps at these temperatures.

To alleviate the reduced effectiveness of FRP systems at elevated temperatures, a novel composite material, namely textile-reinforced mortar (TRM) has been proposed during the last decade for strengthening concrete elements (Koutas *et al.* 2019). TRM combines advanced fibres in form of textiles (with open-mesh configuration) with inorganic matrices, such as cement-based mortars. The same class of materials is also referred to in the literature as FRCM (e.g. Carloni *et al.* 2015). The effectiveness of TRM as a strengthening material has been investigated in a number of studies (i.e. Triantafillou and Papanicolaou 2006, Papanicolaou *et al.* 2008, Tetta *et al.* 2015, Tetta *et al.* 2016, Raoof *et al.* 2016 and Koutas and Bournas 2016) and found to be comparable to FRP systems in many respects. TRM confinement was very effective in enhancing the strength and deformability of concrete and RC columns (Triantafillou *et al.* 2006), but also their deformation capacity under seismic loading (Bournas *et al.* 2007, 2009). Moreover TRM jacketing has been recently combined with thermal insulation materials for the concurrent seismic and energy retrofitting of the building envelopes (Triantafillou *et al.* 2017, Bournas 2018, Gkournelos *et al.* 2019, Pohoryles *et al.* 2020)

TRM composites appear to be non-combustible nor flammable and are expected to outperform FRPs at high temperatures. Nonetheless, the behaviour of TRM vs. FRP systems at elevated temperature or fire has not been investigated yet sufficiently, due to the experimental difficulties that exist in applying simultaneously loading and elevated temperatures or fire to the tested specimens. Hence, the majority of studies identified in the literature were concentrated on either the mechanical (tensile stress-strain) behaviour of TRM composites, or on examining the residual capacity of TRM as a

strengthening material of RC/masonry structural elements (e.g. Al-Salloum *et al.* 2016, Donnini *et al.* 2016, Maroudas and Papanicolaou 2017, Papanicolaou *et al.* 2008, Triantafillou *et al.* 2017, Tlajji *et al.* 2018, Truong *et al.* 2018, Messori *et al.* 2019, Askouni *et al.* 2019, Kapsalis *et al.* 2019).

There are only a few studies reported in the literature on TRM versus FRP as strengthening materials at high temperature, namely those of Bisby *et al.* 2013, Tetta and Bournas 2016 and Raoof and Bournas 2017a, b. Bisby *et al.* 2013 undertook flexural strengthening of RC beams. Both un-retrofitted and strengthened beams were tested up to failure at ambient temperature, and their counterpart specimens were tested under sustained load while being exposed to increasing elevated temperature. In specimens tested at high temperature, the critical-anchorage zones were kept cool (presuming that debonding of heated anchorage zones is prevented through insulation or by mechanical means). Tetta and Bournas 2016 investigated the performance of TRM vs FRP at high temperature in shear strengthening of medium and full-scale RC beams, concluding that TRM is much more effective than FRP in increasing shear capacity of RC beams subjected to various high temperatures (100 °C, 150 °C, and 250 °C). Raoof and Bournas 2017a investigated the bond performance between the TRM vs FRP and concrete interfaces at ambient and high temperatures. In steady state tests, TRM specimens maintained an average of 85% of their ambient bond strength up to 400 °C, whereas the corresponding value for FRP specimens was only 17% at 150 °C. In transient test condition, TRM also outperformed over FRP in terms of both the time they maintained the applied load and the temperature reached before failure. Finally, Raoof and Bournas 2017b explored the flexural behaviour of RC beams strengthened with TRM and FRP composites at ambient and high temperatures. TRM maintained an average effectiveness of 55%, compared to its effectiveness at 20 °C, contrary to FRP which totally lost its effectiveness when subjected at high temperature.

In an effort to develop strengthening systems with enhanced performance at elevated temperatures, this paper investigates, for the first time, the performance and effectiveness of both FRP and TRM confining materials of concrete *at elevated temperatures*, such as would be experienced during a fire, when the confining system is *active under sustained load*; this was done by testing concrete cylinders with different amounts of FRP or TRM confinement at various temperatures. The main objective was to develop an understanding of the confining mechanisms at elevated temperature and to suggest defensible limiting temperatures for FRP and TRM strengthening systems in fire.

## EXPERIMENTAL PROGRAM

The main objective of the experimental program was to provide a better understanding on the effectiveness of TRM versus FRP confinement of concrete at ambient and elevated temperatures. The investigation was carried out on cylindrical specimens. The investigated parameters considered include, the use of inorganic mortar versus resin-based matrix material for the textile reinforcement

(TRM vs. FRP), the number of textile layers (one or three) and the increase of temperature (from ambient to 400°C, with the tests performed under a steady-state thermal regime *at* elevated temperature).

Thirty tests were performed on normal strength concrete cylinders that were loaded at both ambient and elevated temperatures. All tests were performed under a steady state thermal regime. Details of the experimental program are given in Table 1. All tests were on 100 mm diameter, 200 mm tall concrete cylinders; this was chosen as it allowed test specimens to fit within a bespoke environmental chamber fitted within a 600 kN materials testing frame. All cylinders were cast in groups of ten in three batches using the same concrete mix design. The compressive strength of concrete was determined firstly from three 150 mm cubes taken during casting of the cylinders. The resulting value for the 28-day average compressive strength was 25 MPa with a standard deviation of 1.7 MPa. Parameters varied within the testing program included the following.

#### ***Type and amount of confinement***

Six cylinders were tested without confinement to determine the unconfined concrete properties and to determine the reductions in concrete properties caused by heating to the maximum exposure temperature used (400°C). Twelve cylinders were wrapped with FRP (six with a single layer and six with three continuous layers), whereas twelve additional cylinders were wrapped with TRM (six with a single layer and six with three continuous layers). Table 1 summarizes the details of all tested specimens.

The same reinforcement was used in both TRM and FRP systems. This reinforcement comprised a textile with equal quantity of high-strength carbon fibres in two orthogonal directions, as shown in Fig. 1a. The weight of the textile was 220 g/m<sup>2</sup>, whereas its nominal thickness (based on the equivalent smeared distribution of fibres) was 0.062 mm. According to the manufacturer datasheets the tensile strength and the modulus of elasticity of the carbon fibres were 4800 MPa and 225 GPa, respectively. It should be noted however, that the use of bi-directional textiles comprising equal quantity of fibres in two orthogonal directions makes little sense in practical confinement applications where the fibres in the longitudinal direction are not needed. In such cases the carbon longitudinal fibres could be replaced with cheap (e.g. polypropylene or glass) and lighter fibres, should the manufacturing of such hybrid textiles becomes affordable in the future

For the specimens receiving mortar as binding material an inorganic binder was used, consisting of Portland cement and polymers at a quite large ratio of 8:1 by weight, for achieving high tensile strength. The water-binder ratio in the mortar was 0.23:1 by weight and in combination with the fine

grained sand (0-0.4mm) resulted in plastic consistency and excellent workability. The strength properties of the mortar (average values of three specimens) was obtained experimentally using prisms of 40x40x160 mm dimensions, according to the EN 1015-11. The 28-day average mortar's compressive and flexural strength were 26.9 MPa and 8.64 MPa, respectively, at ambient temperature. Mortar prisms were also tested at various elevated temperatures. The prisms were fixed in the furnace, heated up to the desired temperature, kept for one hour at this temperature, and then tested according to the EN 1015-11 specifications. This procedure was repeated for various temperatures, and Fig. 1b illustrates the mortar flexural and compressive strength versus temperature curve. For the specimens receiving epoxy adhesive as binding material, a commercial adhesive (two-part epoxy resin Sikadur 330, with a mixing ratio 4:1 by weight) was used with an elastic modulus of 3.8 GPa and a tensile strength of 30 MPa (according to the manufacturer datasheets). It is noted that, in general the temperature behavior of the adhesive is strongly affected by the type of epoxy under consideration (e.g. Saafi 2002, Signorini *et al.* 2020). Tests for the epoxy used are presented in the following section.

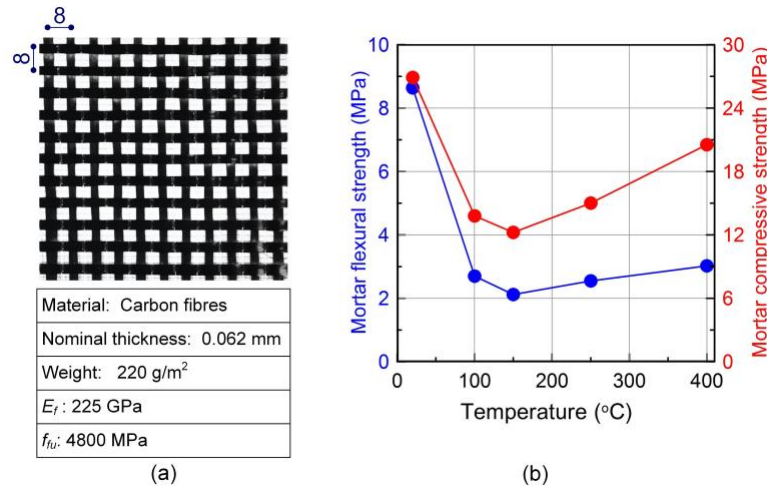


Figure 1 (a) Carbon-fibre textile material used in this study; (b) Mortar flexural and compressive strength versus temperature curve.

For FRP-jacketed specimens the first textile layer was applied on the top of the first resin layer and was then impregnated in-situ with resin using a plastic roll. Special care was taken to ensure the full impregnation of the textile fibres with resin. When three textile layers were to be applied, the process was repeated until the application of all the layers was completed. For TRM-jacketed specimens the mortar was applied in approximately 2 mm-thick layers with a smooth metal trowel. After application of the first mortar layer (Fig. 2a) on the (wetted) concrete surface, the textile was applied and pressed slightly into the mortar, which protruded through all the perforations between the fibre rovings (Fig. 2b). The next mortar layer covered the textile completely, and the operation was repeated until all textile layers were applied and covered by mortar (Fig. 2c). Application of each mortar layer occurred while the previous layer was still in a fresh state. No wrap overlap was provided vertically.

### Thermal Exposure

Temperatures were chosen in the range of the  $T_g$ , as determined from Dynamic Mechanical Analysis (DMA) and the decomposition temperature ( $T_d$ , as determined from thermogravimetric analysis) of the epoxy adhesive. The epoxy resin used in the current study has a  $T_g$  of 58°C based on tan delta peak from DMA testing. Samples were heated without any applied load at a heating rate of 10°C/min until the target temperature was reached. To assure a uniform sample temperature all samples were then held at the target testing temperature for 60 minutes before testing.

Table 1 Details of the Experimental Program

| No.                              | Wrapping               | Matrix/<br>Adhesive | Exposure<br>Temp. (°C)               | Comments   |
|----------------------------------|------------------------|---------------------|--------------------------------------|--|
| 1<br>2                           | --                     | --                  | 20                                   | Control tests on unconfined concrete at ambient (with repeat test)   |
| 3<br>4<br>5<br>6                 |                        |                     | 100<br>150<br>200<br>400             | Control tests on unconfined concrete at elevated temperature   |
| 7<br>8<br>9<br>10<br>11<br>12    | Single layer<br>of FRP | Epoxy               | 20<br>80<br>100<br>150<br>200<br>400 | FRP confined concrete at ambient<br>Temperatures in the range of $T_g^*$<br>Temperatures well above $T_g^*$<br>Temperature in the range of $T_d^{**}$                          |
| 13<br>14<br>15<br>16<br>17<br>18 |                        |                     | 20<br>100<br>150<br>200<br>400       | TRM confined concrete at ambient<br>Single layer of TRM at various temperatures<br>Repeat test at 400°C  |
| 19<br>20<br>21<br>22<br>23<br>24 | Three layers<br>of FRP | Epoxy               | 20<br>100<br>150<br>200<br>400       | FRP confined concrete at ambient<br>Repeat test at ambient<br>Temperature in the range of $T_g^*$<br>Temperatures well above $T_g^*$<br>Temperature in the range of $T_d^{**}$ |
| 25<br>26<br>27<br>28<br>29<br>30 |                        |                     | 20<br>100<br>150<br>200<br>400       | TRM confined concrete at ambient<br>Three layers of TRM at various temperatures<br>Repeat test at 400°C  |

\*  $T_g$  – epoxy glass transition temperature; \*\* $T_d$  – epoxy decomposition temperature

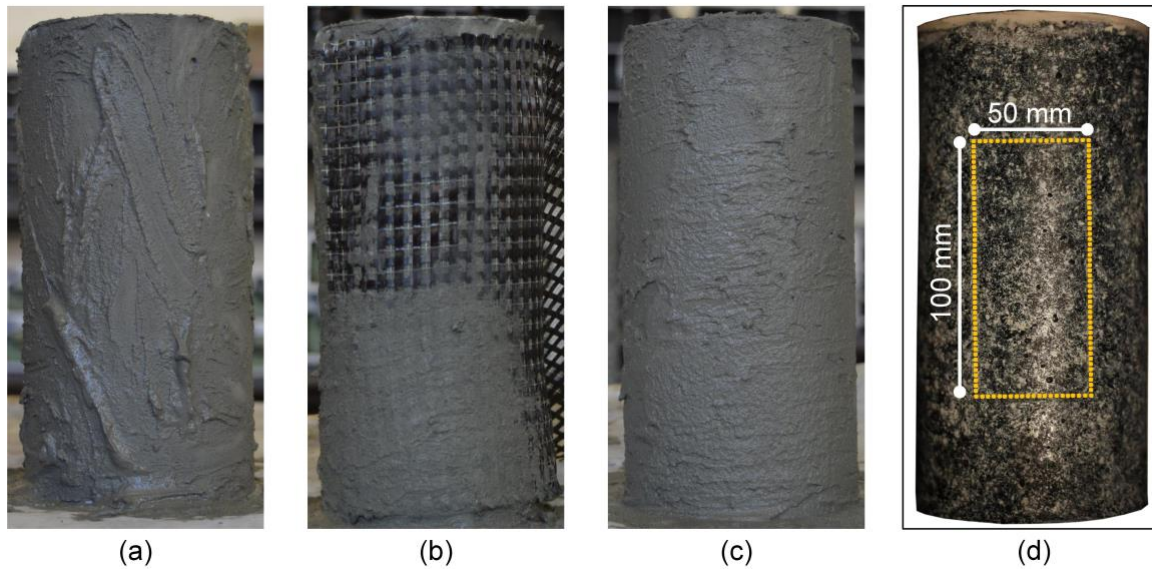


Figure 2 (a) Application of the first layer of mortar; (b) application of the first layer of textile layer into the mortar; (c) application of the final layer of mortar; (d) “strain rectangle” used to calculate hoop and axial strains.

All samples were tested in an Instron 600LX testing frame with an integrated environmental chamber at a loading rate of 1mm/min (crosshead displacement) until failure. Axial and hoop strains were measured using image correlation analysis via digital images captured every 5 seconds during testing with post-testing analysis performed in GeoPIV software (White *et al.* 2003). Full details of the image analysis technique have been presented for similar testing by Rickard *et al.* 2013. Temperatures were monitored during testing by a single thermocouple for gas phase temperature within the chamber (placed next to the sample) and a single thermocouple mounted on the surface of the sample at mid-height. Testing occurred at least 180 days after casting the concrete so as to ensure that the concrete had cured sufficiently to avoid explosive concrete spalling during heating (based on the experience of the authors). The test setup is shown in Fig. 3.



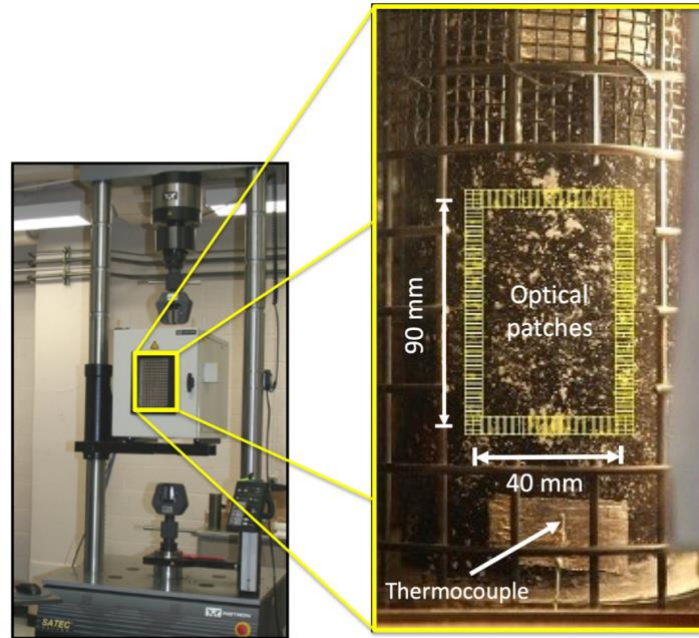


Figure 3 Test set-up used for the compression tests at elevated temperatures

The monitoring area of all specimens was painted with a high contrast texturing effect using black paint with a random white speckle pattern; this was to enable the use of digital image correlation for strain measurement during testing. Strains were measured using a “strain rectangle” as shown in Fig. 2d. Hoop strains were measured as the average of 50 virtual strain gauges distributed over the height of the middle 90mm of the specimens, each with a gauge length of 40mm. Axial strains were measured as the average of 20 virtual strain readings distributed over the width of the middle 40mm of the specimens’ diameter, each with a gauge length of 90mm. More details on this strain measurement approach can be found in Bisby *et al.* (2011).

#### ***Ancillary Tensile tests on TRM and FRP coupons***

Three tensile TRM and FRP coupons with the geometry shown in Fig. 4a and 4c, respectively, were fabricated and tested to characterize the tensile behavior of the composite (TRM or FRP) materials. Uniaxial tensile testing was carried out using a 200 kN universal testing machine at a monotonic loading rate of 0.02 mm per second. Two LVDTs (one on each side of the specimens) were attached to the coupons to record their axial displacement during testing, as shown in Fig. 4b and 4d for TRM and FRP specimens, respectively. More details on these test set-ups are given by Tetta *et al.* 2018.

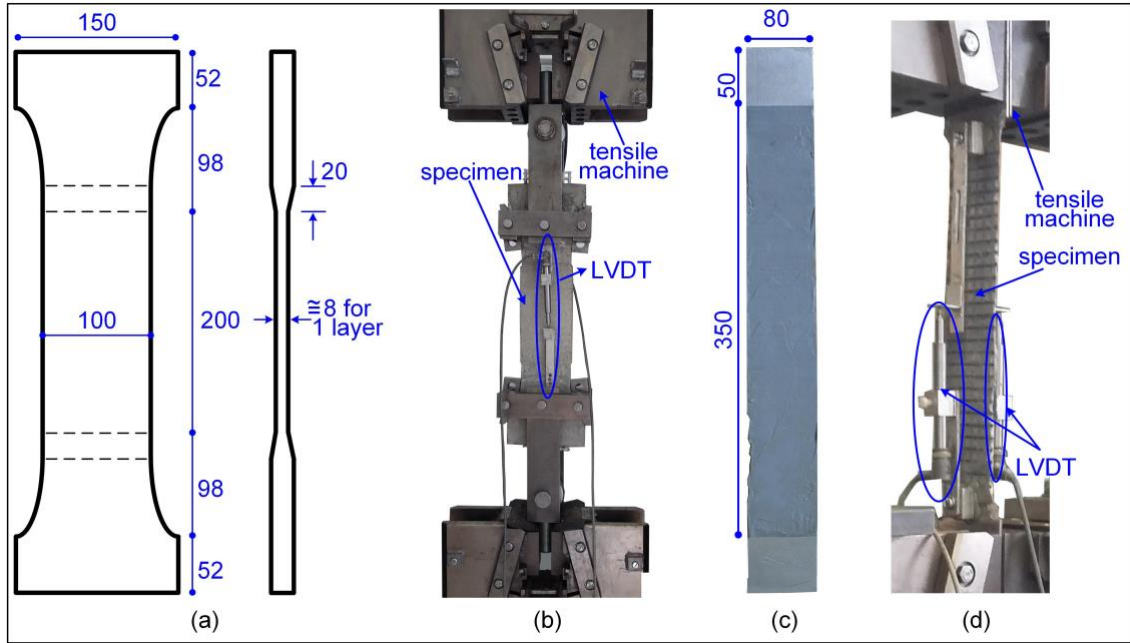


Figure 4 (a) Geometry of TRM coupons; (b) test set-up for tensile testing of TRM coupons; (c) geometry of FRP coupons; (b) test set-up for tensile testing of FRP coupons

The mean values of ultimate tensile stress ( $f_{tu}$ ), ultimate tensile strain ( $\epsilon_{fu}$ ) and the modulus of elasticity of ( $E_f$ ) for both TRM and FRP coupons are presented in Table 2 (the standard deviation is also given in parentheses).

Table 2 Summary of test results of both TRM and FRP coupons

|             | Ultimate tensile strength, $f_{tu}$ (MPa) | Ultimate tensile strain, $\epsilon_{fu}$ (%) | Modulus of elasticity, $E_f$ (GPa) |
|-------------|---|--|------------------------------------|
| TRM coupons | 1545 (132)                                | 0.798 (0.095)                                | 182.6 (21)                         |
| FRP coupons | 2802 (76)                                 | 1.314 (0.11)                                 | 213.3 (16)                         |

## EXPERIMENTAL RESULTS AND DISCUSSION

Summary plots showing the results of all tests listed in Table 1 are given in Fig. 5, and numerical summaries of the tests are presented in Table 3. They include: the wrapping configuration for each specimen; the target temperature to which the sample was exposed during testing; both air and surface temperature at failure; the peak load; the peak stress,  $f_{cc}$ ; the observed failure mode; the jacket confining effectiveness in terms of strength,  $f_{cc}/f_{cc,0}$  (the ratio of the peak stress sustained by the confined concrete cylinder divided by the concrete-only strength of the control cylinder at ambient temperature); and the effectiveness of TRM vs FRP jackets in terms of strength,  $f_{cc}/f_{cc,R}$ .

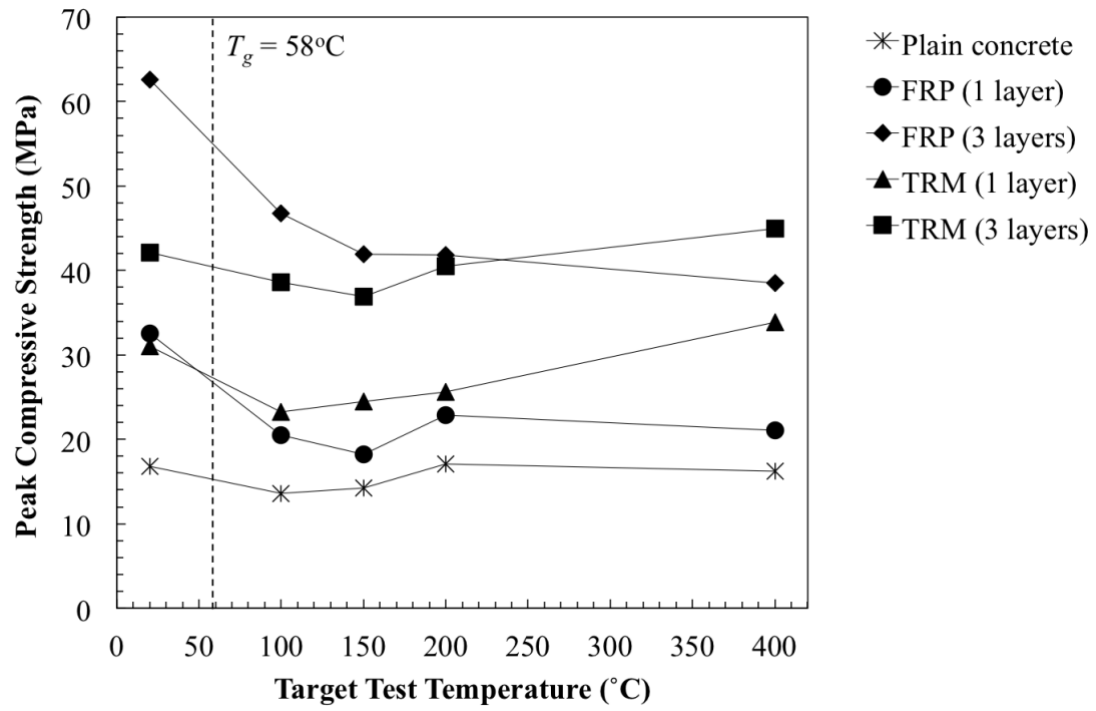


Figure 5 Ultimate Compressive Strength versus Temperature

Table 3 Summary of Test Results

| No.  | Wrapping            | Target Exposure Temp.(°C) | Temp. at Failure (°C) |         | Peak Load (kN) | Peak Stress, $f_{cc}$ (MPa) | Failure Mode* | $f_{cc}/f_{co}$ | $f_{cc}/f_{cc,R}$ |
|--|---------------------|---------------------------|-----------------------|---------|----------------|-----------------------------|---------------|-----------------|-------------------|
|  |                     |                           | Air                   | Surface |                |                             |               |                 |                   |
| 1  | --                  | 20                        | 20                    | 20      | 132.0          | 16.1                        | --            | 1               | NA                |
| 2  |                     |                           | 20                    | 20      | 121.2          | --                          |               |                 |                   |
| 3  |                     | 100                       | 99                    | 96      | 107.2          | 13.6                        | --            | 1               | NA                |
| 4  |                     | 150                       | 150                   | 139     | 111.4          | 14.2                        | --            | 1               | NA                |
| 5  |                     | 200                       | 200                   | 189     | 134.3          | 17.1                        | --            | 1               | NA                |
| 6  |                     | 400                       | 400                   | 362     | 127.3          | 16.2                        | --            | 1               | NA                |
| 7  | Single layer of FRP | 20                        | 20                    | 20      | 255.1          | 32.5                        | Rupture       | 2.02            | 1                 |
| 8  |                     | 80                        | 76                    | 74      | 220.2          | 28.0                        | Rupture       | NA              | NA                |
| 9  |                     | 100                       | 94                    | 93      | 161.1          | 20.5                        | Mixed         | 1.27            | 1                 |
| 10   |                     | 150                       | 148                   | 145     | 142.6          | 18.2                        | Mixed         | 1.13            | 1                 |
| 11   |                     | 200                       | 196                   | 186     | 179.6          | 22.9                        | Adhesive      | 1.42            | 1                 |
| 12   |                     | 400                       | 394                   | 370     | 165.6          | 21.1                        | Adhesive      | 1.31            | 1                 |
| 13   | Single layer of TRM | 20                        | 20                    | 20      | 243.1          | 31.0                        | Rupture       | 1.92            | 0.95              |
| 14   |                     | 100                       | 94                    | 93      | 182.3          | 23.2                        | Rupture       | 1.44            | 1.13              |
| 15   |                     | 150                       | 146                   | 143     | 192.8          | 24.5                        | Mixed         | 1.52            | 1.35              |
| 16   |                     | 200                       | 195                   | 186     | 201.4          | 25.6                        | Rupture       | 1.59            | 1.12              |
| 17   |                     | 400                       | 377                   | 369     | 266.4          | 31.5                        | Mixed         | 1.95            | 1.49              |
| 18   |                     |                           | 386                   | 375     | 227.5          |                             | Rupture       |                 |                   |
| 19   | Three layers of FRP | 20                        | 20                    | 20      | 491.6          | 62.8                        | Rupture       | 3.89            | 1                 |
| 20   |                     |                           | 20                    | 20      | 494.0          |                             | Rupture       |                 |                   |
| 21   |                     | 100                       | 93                    | 91      | 367.4          | 46.8                        | Rupture       | 2.90            | 1                 |
| 22   |                     | 150                       | 147                   | 139     | 328.9          | 41.9                        | Mixed         | 2.60            | 1                 |
| 23   |                     | 200                       | 195                   | 188     | 328.1          | 41.8                        | Adhesive      | 2.59            | 1                 |
| 24   | 400                 | 384                       | 371                   | 302.2   | 38.5           | Adhesive                    | 2.39          | 1               |                   |
| 25   | Three layers of TRM | 20                        | 20                    | 20      | 330.5          | 42.1                        | Rupture       | 2.61            | 0.67              |
| 26   |                     | 100                       | 93                    | 89      | 303.1          | 38.6                        | Mixed         | 2.39            | 0.82              |
| 27   |                     | 150                       | 146                   | 141     | 290.1          | 36.9                        | Rupture       | 2.29            | 0.88              |
| 28   |                     | 200                       | 194                   | 186     | 317.8          | 40.5                        | Rupture       | 2.51            | 0.97              |
| 29   |                     | 400                       | 396                   | 371     | 353.7          | 45                          | Mixed         | 2.79            | 1.17              |
| 30   |                     |                           | 383                   | 362     | 353.1          |                             | Mixed         |                 |                   |
| * ‘Rupture’ refers to failure by tensile rupture of the confining material in the hoop direction, ‘Adhesive’ refers to failure by within the adhesive layer, and ‘Mixed’ refers failure by a combination of rupture and adhesive failures. |                     |                           |                       |         |                |                             |               |                 |                   |

### Unconfined Concrete Cylinders Tests

Six unwrapped (plain) concrete cylinders were tested. Two were tested to define ambient strength, and the remaining four were tested at selected elevated temperatures (100°C, 150°C, 200°C and 400°C) in order to assess the effects of elevated temperature on the strength and stiffness of the unconfined

concrete; such that any strength reductions observed for the FRP and TRM confined specimens could be attributed to reductions in the effectiveness of the confining mechanism. The average ambient unwrapped concrete strength was 16.1 MPa. The concrete strength was reduced slightly, by 15% and 12% at 100°C and 150°C, respectively, before recovering to a strength 5% above that at ambient at 200°C. At 400°C there was no obvious reduction in compressive strength. In addition the failure mode of unwrapped concrete cylinders was not affected from their exposure at elevated temperature, as shown in Fig. 6a and b. Whilst it is difficult to draw definitive conclusions regarding the effects of elevated temperature exposure on the plain concrete cylinders due to the small number of specimens tested, it is noteworthy both that these test data contradict the widely accepted concrete strength reductions with temperature suggested in the Structural Eurocodes (CEN, 2004) – which indicates an expected compressive strength reduction of between 15 and 20% at 400°C, depending on the aggregate mineralogy – and that similar strength trends seem to underlie the responses of the FRP and TRM confined specimens (discussed below). The lack of reduction in compressive strength of the concrete at 400°C suggests that additional research is warranted in this area.

### ***Tests on FRP Confined Concrete***

Figure 5 and Table 3 show a clear trend of reducing FRP confined concrete strength with increased steady state exposure temperature; although with such a small number of samples it is difficult to clearly distinguish if this is attributed to concrete thermal damage effects and/or loss of FRP confinement effects. Whilst the results for FRP confined cylinders are similar to those previously reported by Rickard *et al.* (2013), additional testing with a larger number of cylinders will be required to have greater statistical confidence in the results obtained.

It is clear that exposure temperatures above  $T_g$  cause considerable reductions in the strength of FRP confined concrete cylinders. It is also clear, however, as previously reported by Rickard *et al.* (2013), that the FRP wrap provided considerable additional strength at all temperatures tested, particularly for the case with three continuous layers of carbon fibre reinforcement. For the case of three layers of FRP, the confinement continued to enhance the failure strength at temperatures well above  $T_g$ . For example, strength was enhanced by more than 200% at 400°C. The confinement provided by the single layer of FRP is considerably less; this is likely the result of frictional bond strength for the three layer wrapping, which is able to provide confinement even once the adhesive has lost the majority of its mechanical properties.

Both specimens with one and three FRP layers failed due to rupture of FRP jacket at ambient temperature as shown in Fig. 6c and d. The same failure mode was observed in all FRP confined cylinders tested up to 80 °C and 100 °C. FRP confined cylinders tested at 150 °C failed due to a mixed

failure mode including both fibre rupture and adhesive failure, as shown in Fig. 6e, whereas the failure of cylinders tested at temperature above 150 °C was attributed to adhesive failure due to softening or decomposition of epoxy resin (Fig. 6f).

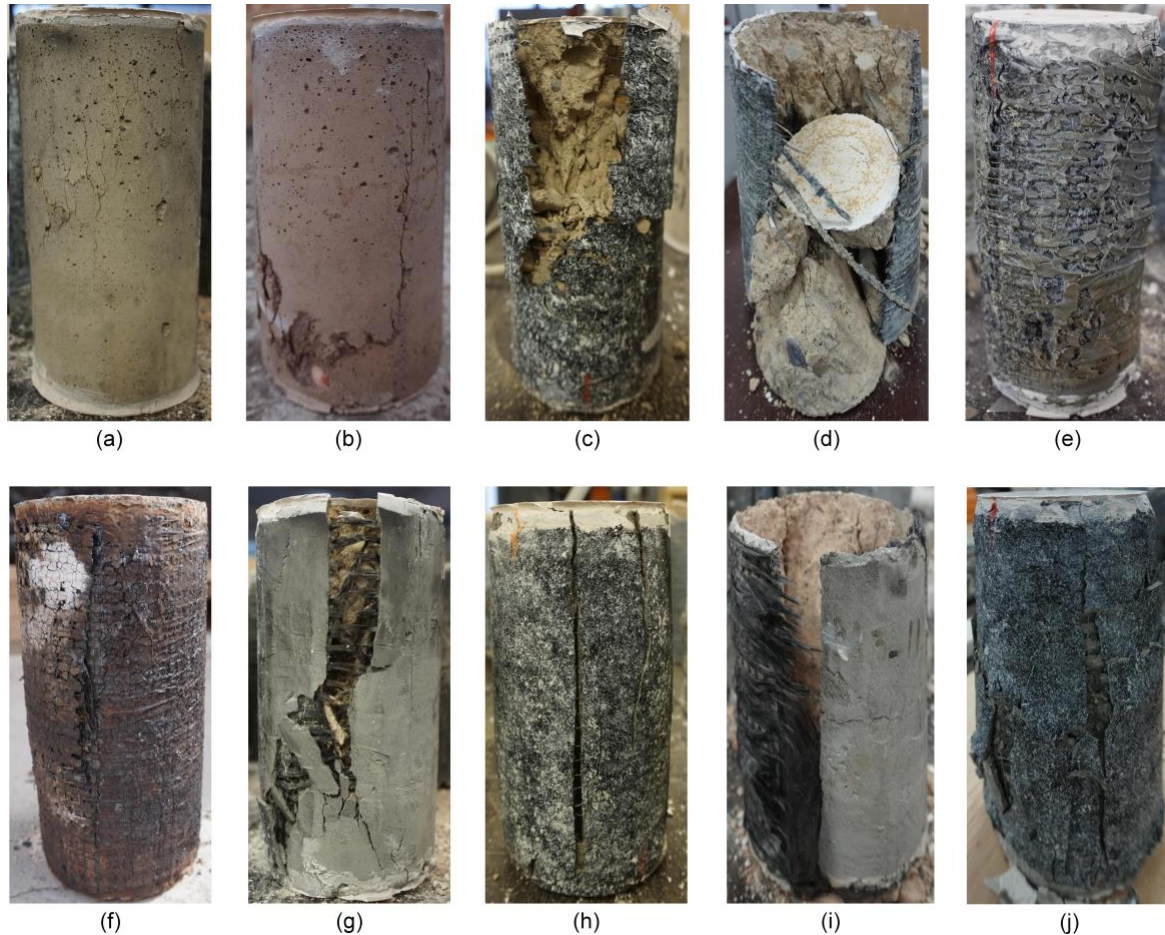


Figure 6 Failure modes of tested specimens: (a) control specimen at ambient temperature; (b) control specimen at 400 °C; (c) single layer of FRP at ambient temperature; (d) three layers of FRP at ambient temperature; (e) single layer of FRP at 400 °C; (f) three layers of FRP at 400 °C; (g) single layer of TRM at ambient temperature; (h) single layer of TRM at 400 °C; (i) three layers of TRM at 400 °C; (j) three layers of TRM at 400 °C.

### ***Tests on TRM Confined Concrete***

For the TRM confined concrete cylinders, Figure 5 and Table 3 show that the TRM system was marginally less effective than the FRP system for a single layer at ambient conditions, and that its performance was similarly affected by exposure to a temperature of 100°C, losing 23% of its strength at this temperature. This is likely due to a combination of reductions in the strength of the concrete itself at this temperature (discussed previously) and the strengthening mortar (see Fig. 1b) combined with reductions in the effectiveness of the confinement (for reasons which remain unknown). Failure of the cylinder that received a single TRM layer was due to rupture of TRM jacket, as shown in Fig. 6g. However, at temperatures above 100°C the TRM system recovered its strength more rapidly than

either the plain or FRP confined specimens, and at 400°C the single layer TRM confined sample tested stronger than its counterpart sample at ambient temperature. Failure of single layer TRM cylinders at elevated temperatures was attributed to rupture of the TRM jacket in hoop tension in most cases (Fig. 6h), whereas the failure of some TRM confined cylinders was attributed to combined rupture with adhesive failure (i.e. at 150°C).

Similar observations can be made regarding the performance of the three layer TRM confining system. In this case the strengthening provided by the TRM system was considerably less, by 33%, than the three layer FRP system, probably because of differences in the observed failure mode – tensile pull-out of the fibres from the cementitious matrix followed by partial fibre fracture in the case of the TRM, compared with tensile fibre fracture over the height of the cylinder in the case of the FRP. Failure of the TRM wrapped specimens was considerably less violent than for the FRP wrapped cylinders, and these absorbed more energy than for the FRP wrapped specimens, particularly at lower temperatures. This may present advantages particularly in seismic strengthening applications.

However, at elevated temperature the three layer TRM system displayed similar response as for the single layer TRM system, with mild reductions in strength at 100, 150, and 200°C (likely for the reasons discussed in the previous paragraph), but a small increase (by 7%) in strength at 400°C as compared with the strength at ambient. At elevated temperatures failure of cylinders wrapped with three TRM layers was attributed either to rupture of the TRM jacket (Fig. 6i), or to a combined rupture with adhesive failure, as shown in Fig. 6j.

Increases in the effectiveness of the TRM system at elevated temperature are striking, particularly for the case of the three-layer TRM system, and may be due to thermal prestressing of the carbon fibres during heating, as has previously been suggested by Rickard *et al.* 2013 for multiple layer FRP confining systems at elevated temperature. Since carbon fibres generally have a slightly negative coefficient of thermal expansion, whereas the concrete core has a positive coefficient of thermal expansion, thermal dilation of the concrete core during heating will develop tensile stresses in the carbon fibre mesh, and provided that bond is maintained (either by adhesion or by winding friction) the wrap will self-prestress, which can be expected to enhance both the strength and stiffness of the TRM confined cylinders. This hypothesis warrants additional research and may indicate that unprotected TRM systems are capable of providing effective (i.e. active) confinement of concrete at temperatures up to and exceeding 400°C (something that epoxy-based FRP systems are less able to do). It should be also mentioned that, based on Fig. 1b, both the flexural and compressive strength of mortar at temperatures ranging between 100 °C and 400 °C follow a similar trend with that of the cylinder compressive strength (Fig. 5). Specifically, the mortar flexural strength at ambient

temperature was 8.64 MPa and but decreased when the mortar was exposed to both 100 °C (2.70 MPa) and 150 °C (2.12 MPa). At 250 °C, however, the mortar's strength started increasing (2.55 MPa), recovering to 3.03 MPa at 400 °C.

### ***Axial/Hoop Stress versus Strain Response***

Typical stress-strain curves obtained during steady state testing using the image correlation analysis are given in Fig. 7. It was challenging to obtain consistent strain information during these tests due to thermal effects on the image correlation technique; the results should therefore be taken as only indicative of the response. It is noteworthy that both the strength and stiffness of the confined concrete appear to be significantly reduced at 150°C, whereas these appear to be recovered at 400°C. Again, this behaviour warrants further investigation, both for confinement research but also for structural fire engineering research focusing on concrete structures.



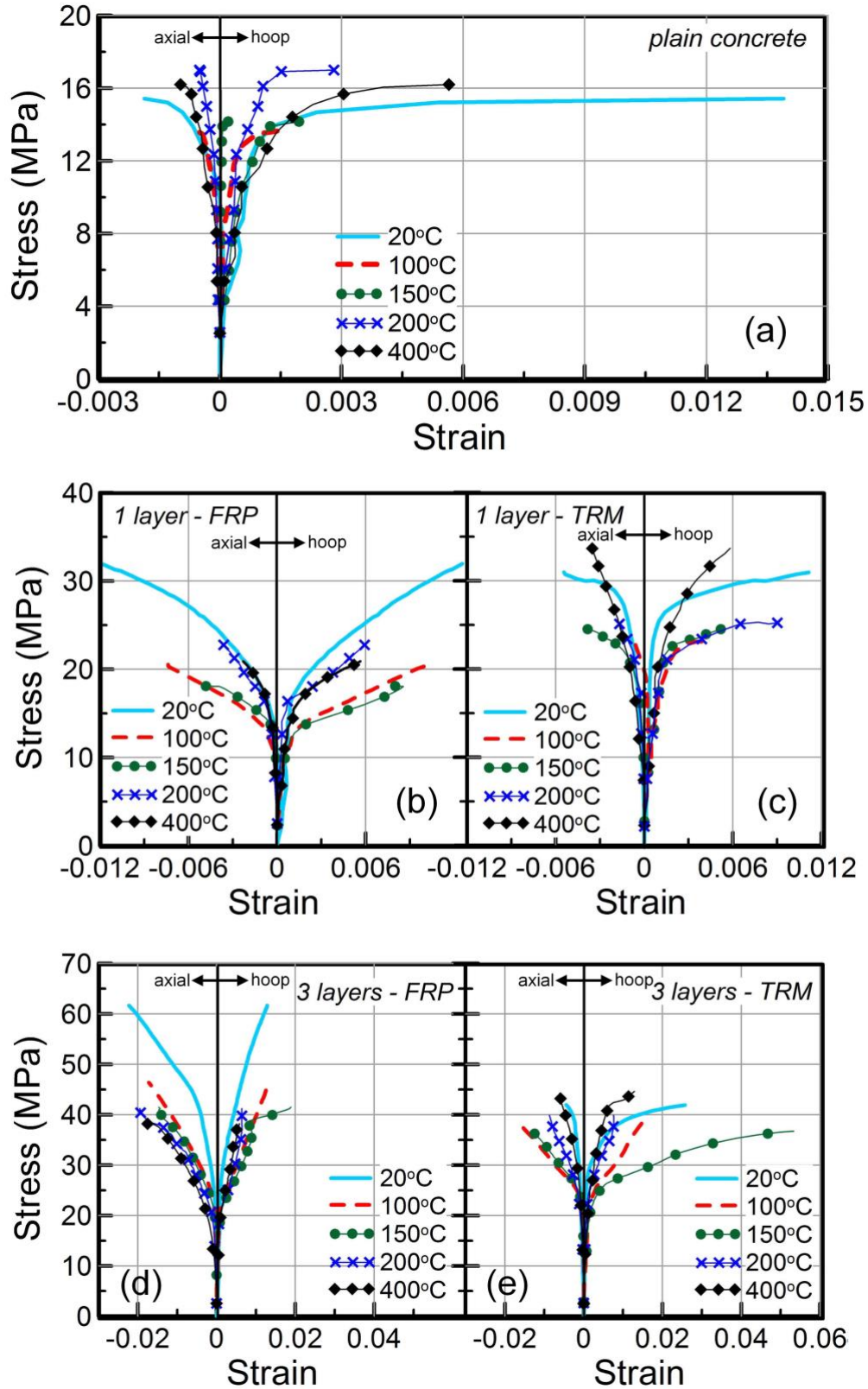


Figure 7 Stress-Strain Curves for: (a) Plain concrete cylinders; (b) cylinders with one FRP layer; (c) cylinders with one TRM layer; (d) cylinders with three FRP layers and (e) cylinders with three TRM layers

### TRM vs FRP Confining Effectiveness

The confining effectiveness in terms of strength,  $f_{cc}/f_{co}$  is given in Table 3. By comparing the response of confined cylinders with that of unjacketed ones, it is concluded that both FRP and TRM confinement is effective in increasing the capacity of plain concrete cylinders. The effectiveness in terms of strength ( $f_{cc}/f_{co}$ ) was approximately 1.92 for a single layer of TRM or 2.02 for a single FRP layer at ambient temperature. Confinement effectiveness decreased with increasing temperature. The single FRP layer had its minimum effectiveness ( $f_{cc}/f_{co}$ ) at 150 °C (1.13), whereas for the single TRM layer this occurred at 100 °C (1.44). In case of three layers, at ambient temperature, the  $f_{cc}/f_{co}$  values were 3.89 and 2.61 for FRP and TRM jacketing, respectively. The minimum jacket confining effectiveness for three FRP layers was 2.39 at 400 °C, whereas the corresponding value for the equivalent TRM system was 2.29 at 150 °C (with subsequent effectiveness recovery as already discussed).

A comparison of the effectiveness of mortar-based jackets to that of resin-based jackets is given by dividing their effectiveness. In terms of strength this is expressed by the ratio  $f_{cc}/f_{cc,R}$  (see Table 3). For a lesser amount of reinforcement (i.e. a single carbon fibre layer) the effectiveness of TRM and FRP was almost equal ( $f_{cc}/f_{cc,R} = 0.95$ ) at ambient temperatures, while at temperatures ranging between 100-200 °C, the TRM confinement became progressively more effective than FRP ( $f_{cc}/f_{cc,R} = 0.95$  ranges from 1.13 to 1.35). At 400 °C TRM was found 1.5 times more effective than FRP in terms increasing the cylinders strength. For higher amount of confinement reinforcement (i.e. 3 carbon fibre layers), the confining effectiveness of TRM was considerably lower than FRP jacketing at ambient temperatures ( $f_{cc}/f_{cc,R} = 0.67$ ). However as can be observed in Table 3, the ratio  $f_{cc}/f_{cc,R}$  is increasing with the temperature in an almost proportional manner, with recorded values equal to 0.82, 0.88, 0.97 and 1.17 for 100 °C, 150 °C, 200 ° and 400 °C, respectively.

### CONCLUSIONS

The following conclusions can be drawn on the basis of the tests reported herein:

- Considerable loss of effectiveness of the FRP wrap system occurred at temperatures exceeding the  $T_g$  of the epoxy adhesive used. This is thought to be due to reductions in the tensile, and more importantly bond, strength and stiffness of the FRP wraps at these temperatures.
- The ultimate load capacity of FRP wrapped cylinders continued to decrease with increasing temperatures; however, the FRP wrap continued to provide some confinement at all exposure temperatures, both for a single layer and for a triple layer, even at 400°C which is well above  $T_g$ . This is possibly attributed to bond retention resulting from winding friction, which appears to be (as expected), much more effective for three continuous layers of FRP than for a single layer.

- FRP rupture was the observed failure mode at temperatures below 100°C; above 100°C the failure mode was observed to transition to bond failure in the FRP overlapping zone.
- Minor loss of effectiveness of the TRM wrap system occurred at temperatures between 100 and 200°C. This is thought to be due to reductions in the compressive strength of the concrete at these temperatures (as corroborated by compression tests on unconfined concrete at these temperatures). However, both single and triple layer TRM wrap systems demonstrated enhanced strength at 400°C.
- It appears that differential thermal expansion between the carbon fibre reinforced wraps (contracting) and the concrete column (expanding) caused a slight prestress of the FRP and TRM systems during heating.
- The number of FRP and TRM layers of wrapping (hence the effective overlap length used) had a significant impact on the confinement effectiveness at elevated temperature; however, additional testing is required to study the influence of wrapping with multiple continuous layers on the performance of FRP and TRM confined concrete at elevated temperature.

## RECOMMENDATIONS

The following are recommendations for future work in this area:

- Further tests on unconfined concrete at elevated temperature are required to better understand the effects of heating (and heating rate) on reduction in unconfined concrete compressive strength.
- Additional repeat tests, particularly on FRP and TRM confined concrete, are required to ensure statistical confidence in the results obtained and to corroborate the results and hypotheses presented herein.
- Other available FRP and TRM wrap systems and materials need to be studied to allow any generalization of the observations made during the current study.
- Cylinders tested in this project were subjected to loads at elevated temperatures for relatively short periods of time. The potential effects of prolonged loading and heating, as might occur in warm service temperatures, require study since creep may cause failure at lower temperatures under long term loading.
- Additional tests should be conducted on FRP and TRM confined RC columns at full-scale, including internal steel reinforcement as would almost certainly exist in practice.

## ACKNOWLEDGEMENTS

The third author acknowledges the JRC Exploratory Research Programme, Project **iRESIST+**, Joint Research Centre, European Commission. The authors gratefully acknowledge the assistance of Dr Saad Raoof in the specimens' preparation.

## CONFLICT OF INTEREST

The authors declare that they have no conflict of interest.

## REFERENCES

- ACI (2008). *440.2R-08 Guide for the Design and Construction of Externally Bonded FRP Systems for Strengthening Concrete Structures*, American Concrete Institute, Farmington Hills, MI.
- Al-Salloum, YA, Almusallam TH, Elsanadedy HM and Iqbal RA. Effect of elevated temperature environments on the residual axial capacity of RC columns strengthened with different techniques. *Construction and Building Materials* 2016;115:345-361.
- Askouni, P.D.; Papanicolaou, C.C.G.; Kaffetzakis, M.I. The Effect of Elevated Temperatures on the TRM-to-Masonry Bond: Comparison of Normal Weight and Lightweight Matrices. *Appl. Sci.* Basel 2019, 9, 2156.
- Barrington, J., Dickson, D., Bisby, L. and Stratford, T. (2011). “Strain Development and Hoop Strain Efficiency in FRP Confined Square Concrete Columns”, *American Concrete Institute SP-49*, 9, 9.1-9.20.
- Bentonex (2016). <http://www.betontex.it/prodotti/schede-tecniche/>, accessed 30<sup>th</sup> May 2019.
- Bisby, L.A., Chen, J.F., Li, S.Q., Stratford, T.J., Cueva, N. and Crossling, K. (2011). “Strengthening fire-damaged concrete by confinement with fibre-reinforced polymer wraps”, *Engineering Structures*, 33(12), pp.3381-3391.
- Bisby L, Stratford T, Hart C, Farren S. Fire Performance of Well-Anchored TRM, FRCM, and FRP Flexural Strengthening Systems. *Advanced Composites in Construction* 2013.
- Bournas, DA., Lontou, PV., Papanicolaou, CG., Triantafillou, TC. (2007). “Textile-reinforced mortar versus fibre-reinforced polymer confinement in reinforced concrete columns”, *ACI Struct J*, 104(6), 740-748.
- Bournas DA, Lontou PV, Papanicolaou CG, Triantafillou TC. Textile-reinforced mortar versus fibre-reinforced polymer confinement in reinforced concrete columns. *ACI Struct J*, 2007;104(6).
- Bournas DA, Triantafillou TC, Zygouris K, Stavropoulos F. Textile-reinforced mortar versus FRP Jacketing in seismic retrofitting of RC columns with continuous or Lap-spliced deformed bars. *J Comp Constr* 2009;13(5):360-371.
- Bournas DA. Concurrent seismic and energy retrofitting of RC and masonry building envelopes using inorganic textile-based composites combined with insulation materials: A new concept. *Compos Part B Eng* 2018;148:166–79
- Carloni C, Bournas DA, Carozzi FG, D’Antino T, Fava G, Focacci F, Giacomini G, Mantegazza G, Pellegrino C, Perinelli C, and Poggi C. Fiber reinforced composites with cementitious (inorganic) matrix. Chapter 9 in: *Design procedures for the use of composites in strengthening of reinforced concrete structures – State of the art report of the RILEM TC 234-DUC*, Eds: C. Pellegrino and J. Sena-Cruz, 2015;349-391, 501 Springer, RILEM STAR Book Series.
- CEN (2004). *EN 1992-1-2:2004 Eurocode 2: Design of concrete structures — Part 1-2: General rules — Structural fire design*, European Committee for Standardisation, Brussels.
- Chowdhury, E., Eedson, R., Green, M., Bisby, L. and Benichou, N. (2011). “Mechanical Characterization of Fibre Reinforced Polymers Materials at High Temperature”, *Fire Tech*, 47, 1063-1080.
- Chowdhury, E., Bisby, L., Green, M. and Kodur, V. (2007). “Investigation of insulated FRP-wrapped reinforced concrete columns in fire”, *Fire Safety J*, 42, 452-460.
- Donnini, J., Corinaldesi, V., Nanni, A. Mechanical properties of FRCM using carbon fabrics with different coating treatments. *Compos. Part B Eng.*, 88 (2016), pp. 220-228, [10.1016/j.compositesb.2015.11.012](https://doi.org/10.1016/j.compositesb.2015.11.012)
- EN 1015-11. Methods of test for mortar for masonry – Part 11: Determination of flexural and compressive strength of hardened mortar, Brussels: Comité Européen de Normalisation; 1993.
- ISOMAT (2016). <http://www.isomat.eu/>. Accessed 30<sup>th</sup> May 2019.
- Gkournelos PD, Bournas DA, Triantafillou TC. Combined seismic and energy upgrading of existing reinforced concrete buildings using TRM jacketing and thermal insulation. *Earthq Struct* 2019;16:625–39. <https://doi.org/10.12989/EAS.2019.16.5.625>.
- Kapsalis, P.; El Kadi, M.; De Vervloet, J.; Munck, M.; Wastiels, J.; Triantafillou, T.; Tysmans, T. Thermomechanical behavior of textile reinforced cementitious composites subjected to fire. *Appl. Sci.* 2019, 9, 747

- Kodur, V., Bisby, L. and Green, M. (2006). "Experimental evaluation of the fire behaviour of insulated fibre-reinforced-polymer-strengthened reinforced concrete columns", *Fire Safety J*, 41, 547-557.
- Koutas L, Bournas DA. Flexural strengthening of two-way RC slabs with textile-reinforced mortar: experimental investigation and design equations. *J Compos Constr*. 2016;doi:10.1061/(ASCE)CC.1943-5614.0000713.
- Koutas LN, Tetta Z, Bournas DA, Triantafillou TC. Strengthening of Concrete Structures with Textile Reinforced Mortars: State-of-the-Art Review. *J Compos Constr* 2019;23:03118001. doi:10.1061/(ASCE)CC.1943-5614.0000882.
- Maroudas, S.R. and Papanicolaou C.G. Effect of high temperatures on the TRM-to-masonry bond, *Key Engineering Materials*, 747, Trans Tech Publ (2017), pp. 533-54.
- Messori, M., Nobili, A., Signorini, C., Sola A. Effect of high temperature exposure on epoxy-coated Glass Textile Reinforced Mortar composites. *Constr. Build. Mater.*, 212 (2019), pp. 765-774.
- Papanicolaou, C.G., Triantafillou, T.C., Papathanasiou, M., Karlos K. Textile-reinforced mortar (TRM) versus FRP as strengthening material of URM walls: out-of-plane cyclic loading *Mater Struct.*, 41 (2008), pp. 143-157.
- Pohoryles DA, Maduta C, Bournas DA, Kouris LA. (2020). Energy Performance of Existing Residential Buildings in Europe: A Novel Approach Combining Energy with Seismic Retrofitting. *Energy and Buildings* (in press).
- Raoof SM, Koutas LN, Bournas DA, Bond between textile-reinforced mortar (TRM) and concrete substrates: Experimental investigation, *Composites Part B* 2016; 98:350-361, doi: 10.1016/j.compositesb.2016.05.041.
- Raoof, S. M., and D. A. Bournas. 2017a. "Bond between TRM versus FRP composites and concrete at high temperatures." *Compos. Part B: Eng.* 127: 150–165. <https://doi.org/10.1016/j.compositesb.2017.05.064>.
- Raoof, S. M., and D. A. Bournas. 2017b. "TRM versus FRP in flexural strengthening of RC beams: Behaviour at high temperatures" *Compos. Part B: Eng.* 154: 424–437. <https://doi.org/10.1016/j.conbuildmat.2017.07.195>
- Rickard, I., Bisby, L., Stratford, T. and Hulsberg, S. (2013). "Effects of Heating on FRP Confinement of Concrete," *11<sup>th</sup> International Symposium on Fibre Reinforced Polymers for Reinforced Concrete Structures*, Guimarães, Portugal, 26-28 June.
- Saafi, M. Effect of fire on FRP reinforced concrete members. *Compos. Struct.* (2002), 58, 11–20.
- Signorini, C., Signorini, A., Nobili, A., Sola, A., Messoric, M. Designing epoxy viscosity for optimal mechanical performance of coated Glass Textile Reinforced Mortar (GTRM) composites." *Construction and Building Materials* 233 (2020): 117325.
- Sika (2016). <http://usa.sika.com/dms/getdocument.get/2b390cda-10e7-3bb5-8295-b9380f89401c/pds-cpd-Sikadur300-us.pdf>, accessed 30th May 2016.
- Tetta ZC, Koutas LN, Bournas DA. Textile-reinforced mortar (TRM) versus fibre-reinforced polymers (FRP) in shear strengthening of concrete beams. *Compos Part B* 2015;77:338-348, doi:10.1016/j.compositesb.2015.03.055.
- Tetta ZC, Koutas LN, Bournas DA. (2016). Shear strengthening of full-scale RC T-beams using textile-reinforced mortar and textile-based anchors. *Compos Part B* 2016;95:225-239, doi:10.1016/j.compositesb.03.076.
- Tetta ZC, and Bournas DA. (2016). TRM versus FRP Jacketing in Shear Strengthening of Concrete Members: Behaviour at High Temperature. *Compos Part B: Eng*, 106, pp. 190-205.
- Tetta ZC, Koutas LN, Bournas DA. (2018). Shear strengthening of concrete members with TRM jackets: effect of shear span-to-depth ratio, material and amount of external reinforcement. *Compos Part B: Eng*, 137, pp. 184-201
- Tlaji, T., Vu, X.H., Ferrier, E. Si Larbi, A. Thermomechanical behaviour and residual properties of textile reinforced concrete (TRC) subjected to elevated and high temperature loading: Experimental and comparative study, *Compos Part B: Eng*, 144 (2018), pp. 99-110, 10.1016/j.compositesb.2018.02.022.
- Triantafillou, T.C., Papanicolaou, C.G. Shear strengthening of reinforced concrete members with textile reinforced mortar (TRM) jackets. *Mater Struct RILEM*, 39 (1) (2006), pp. 85-93

- Triantafillou TC, Papanicolaou CG, Zissimopoulos P, Laourdekis T. Concrete confinement with textile-reinforced mortar jackets. *ACI Struct J* 2006;103(1):28-37.
- Triantafillou TC, Karlos K, Kefalou K, Argyropoulou E. An innovative structural and energy retrofitting system for URM walls using textile reinforced mortars combined with thermal insulation: Mechanical and fire behavior. *Constr Build Mater* (2017);133:1–13. <https://doi.org/10.1016/j.conbuildmat.2016.12.032>
- Truong, G.T., Kim, J., Choi, K.-K. Effect of multi-walled carbon nanotubes (MWCNTs) and electroless copper plating on tensile behavior of carbon fiber reinforced polymers. *Adv. Mater. Sci. Eng.*, 2018 (2018). <https://doi.org/10.1155/2018/8264138>
- White, D., Take, W.A. and Bolton, M. (2003). “Soil deformation measurement using particle image velocimetry (PIV) and photogrammetry”, *Geotechnique*, 53, 619-631.